JOURNAL OF SOLID STATE CHEMISTRY 84, 93–101 (1990)

The Structural Phase Transition in the RECu6 Compounds (RE = La, Ce, Pr, Nd)*

M. L. VRTIS†

Department of Physics and Astronomy, Northwestern University, Evanston, Illinois 60201

AND J. D. JORGENSEN AND D. G. HINKS

Materials Science Division, Argonne National Laboratory, Argonne, Illinois 60439

Received July 11, 1989

The structure of the $RECu_6$ compounds (where RE = La, Ce, Pr and Nd) has been studied using time-of-flight neutron powder diffraction at temperatures ranging from 10 to 573 K. The compounds exhibit a temperature-dependent distortion of the high-temperature orthorhombic cell to a monoclinic one with transition temperatures between 151 and 455 K depending on the rare earth ion. The space groups and the temperature dependence of the monoclinic strain are consistent with a second-order transition driven by a soft acoustic phonon mode. Since the lanthanum compound with no 4*f* electron also exhibits the same transition, it is unlikely that electronic effects involving the 4*f* shell are responsible for the transition observed in these materials.

Introduction

Individually, the intermetallic $RECu_6$ compounds are interesting because of their distinctive and unusual low-temperature properties. $CeCu_6$ has recently attracted much attention because it exhibits low-temperature behavior characteristic of the heavy fermion systems. In particular, the electronic specific heat, $\gamma(0)$, achieves a value of about 1.5 J/mole K^2 (*1–3*) and the magnetic susceptibility, χ, exhibits a crossover from a Curie–Weiss behavior at high temperature to a Pauli-like behavior at low temperature attaining a large finite value of approximately 0.03 emu/mole (*3–5*). In addition, the resistivity of this compound drops dramatically below 10 K, exhibiting a T^2 behavior below ~0.15 K (*6–9*). The interest in $PrCu_6$ lies in its low-temperature-enhanced nuclear spin ordering, occurring at 2.5 mK, as deduced from resistivity (*10*) and specific heat (*11*) measurements. At temperatures below ~6 K, $NdCu_6$ exhibits metamagnetic behavior with four discontinuous steps in its magnetization curve at magnetic fields between 24 and 90 kOe (*12*). $LaCu_6$ serves as a nonmagnetic reference for all the $RECu_6$

* Work supported by the U.S. Department of Energy, BES-Materials Sciences, under Contract W-31-109-Eng-38.

† Present address: Institut Laue-Langevin, 156X, 38042 Grenoble, France.

0022-4596/90 $3.00

compounds, demonstrating those physical properties which are not due to the 4*f* electrons in these compounds (*13*).

Much of the work on the low-temperature aspects of these compounds has been done under the assumption that the low-temperature structure of these materials is the same as at room temperature. Except in the case of $LaCu_6$, this is not true. The room-temperature structure of $LaCu_6$ has been previously reported to be monoclinic $P2_1/c$ (*14*). Recently, two single crystals of $LaCu_6$ have been studied above room temperature and they undergo a structural phase transition to a high temperature, orthorhombic *Pnma* structure with transition temperatures at 527 and 460 K (*15*) for the two different crystals. $CeCu_6$ and $PrCu_6$ are known to exhibit the same structural transition but at much lower temperatures. The transition temperature for $CeCu_6$ has been measured by various authors (*16–20*), who reported values ranging from 168 (*16*) to 220 K (*19*) with large discrepancies due to sample variation. Detailed neutron powder diffraction studies of the structural aspects of the transitions in $CeCu_6$ (*20*) and in $PrCu_6$ (*21*) have also been reported.

The purpose of the present work was to determine the structural phase transition temperature in powder samples of $RECu_6$ where internal strains have largely been removed and to examine the variation of the transition temperature with respect to the rare earth ion. The neutron powder diffraction results show that the monoclinic structure occurs at temperatures below about 455, 214, 206, and 151 K in the rare earth compounds $LaCu_6$, $CeCu_6$, $PrCu_6$, and $NdCu_6$, respectively. By comparison of the transition temperatures in these compounds, we infer that the cerium and possibly praseodymium ions in these compounds possess a slightly different valence than the lanthanum and neodymium ions.

Experimental Details

Samples of $LaCu_6$, $CeCu_6$, and $PrCu_6$ were grown as large ingots pulled from an inductively heated melt contained in a tungsten crucible. The sample of $NdCu_6$ was arc melted from its constituents. Each sample was then crushed to a fine powder and approximately 25 g was sealed in a vanadium container with 1 atm of helium exchange gas for the neutron diffraction measurements.

Neutron powder diffraction data were collected on the special environment powder diffractometer (SEPD) and on the general purpose powder diffractometer (GPPD) (*22*) at Argonne's Intense Pulsed Neutron Source. The samples were cooled by a Displex (Air Products and Chemicals, Inc.) closed cycle helium refrigerator. To search for the phase transition in $LaCu_6$, which occurs above room temperature, two different furnaces were employed to heat the sample. Table I lists the sample conditions for data collection. Data were accumulated at each temperature for about 4 hr on the SEPD and for about 6 hr on the GPPD.

All data were analyzed using the Rietveld structural refinement technique (*23*). For each compound, the high-temperature data were refined in the orthorhombic *Pnma* space group. The temperature range of data collection for the orthorhombic phase of each compound is given in column 4 of Table I. Initial atom positions and lattice constants were obtained either from the literature (as in the case of $CeCu_6$ (*24*)) or from estimates on the refinements of the previous compounds. The refined structural parameters agreed well with those previously reported for $CeCu_6$ (*24, 25*), $PrCu_6$ (*21*), and $LaCu_6$ (*14, 15*). A portion of the raw data and the calculated Rietveld profile for $CeCu_6$ at 295 K is shown in Fig. 1a.

TABLE I

SAMPLE CONDITIONS AND TEMPERATURE RANGE FOR THE DATA COLLECTED ON $RECu_6$ COMPOUNDS

Sample (1)	Instrument (2)	Environment (3)	Data collection in monoclinic phase (4)	Data collection in orthorhombic phase (5)
$LaCu_6$	SEPD	Displex	15–300 K	
		Furnace 1	305–448 K	483–500 K
		Furnace 2	301–448 K	483–573 K
$CeCu_6$	SEPD	Displex	10–200 K	250–295 K
$PrCu_6$	SEPD	Displex	15–200 K	250–295 K
$NdCu_6$	GPPD	Displex	10–125 K	150–300 K

Note. The data were refined using either the monoclinic $P2_1/c$ space group or the orthorhombic *Pnma* space group.

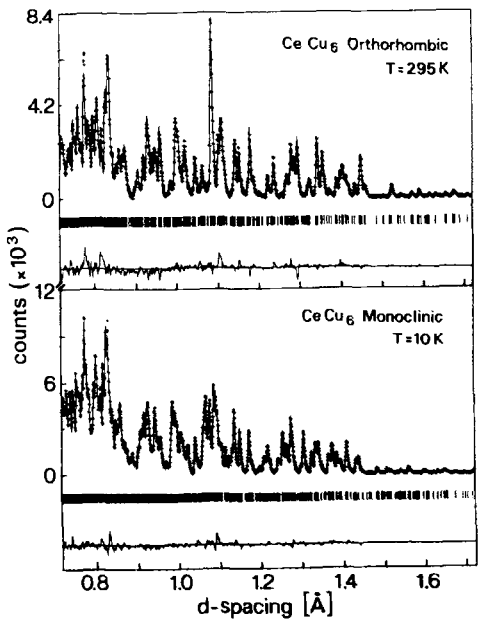

FIG. 1. Portion of the raw time-of-flight neutron powder diffraction data (crosses) and best-fit Rietveld least-squares-fitted diffraction profile (solid line) for $CeCu_6$. Tick marks under the profile indicate the positions of all the allowed Bragg peaks. A difference plot (observed minus calculated intensity) appears at the bottom of the plot. Background has been subtracted prior to plotting. (a) Using an orthorhombic *Pnma* model for $CeCu_6$ at 295 K; (b) using a monoclinic $P2_1/c$ model for $CeCu_6$ at 10 K.

At lower temperatures, a gradual splitting of the Bragg peaks was observed in the raw data after passing through the transition into the monoclinic phase. The monoclinic space group $P2_1/c$ (a subgroup of *Pnma*) was used to refine the data in the low-temperature region. The temperature range of data collection for the monoclinic phase of each compound is listed in column 5 of Table I. No stable convergence in the Rietveld fits could be obtained for four data sets collected on $LaCu_6$ in the immediate vicinity of the transition. A portion of the raw data and the calculated Rietveld profile for $CeCu_6$ at 10 K is shown in Fig. 1b.

The refinement in the orthorhombic phase for data taken on the SEPD included about 700 allowed reflections with *d*-spacings from 0.69 to 2.66 Å. In the monoclinic phase, the total number of allowed reflections increased to about 1250 for nominally the same data range. The data for $NdCu_6$, taken on the GPPD, included about 800 allowed reflections in the orthorhombic phase and about 1450 allowed reflections in the monoclinic phase with *d*-spacings from 0.67 to 2.42 Å. Table II lists the lattice parameters at each temperature according to compound. Table III gives full structural parameters at the highest and lowest tem-

TABLE II

UNIT CELL PARAMETERS OF THE $RECu_6$ COMPOUNDS VS TEMPERATURE

T(K)	a(Å)	b(Å)	c(Å)	β(deg.)	V(Å^3)	R_{wp}	R_{exp}
$LaCu_6$							
15	5.1364(1)	10.1763(2)	8.1072(1)	92.186(1)	423.450(9)	5.36	2.78
50	5.1365(1)	10.1773(2)	8.1084(1)	92.148(2)	423.591(9)	5.35	2.76
100	5.1376(1)	10.1814(2)	8.1136(1)	92.063(2)	424.130(9)	5.39	2.71
150	5.1395(1)	10.1877(2)	8.1207(1)	91.958(2)	424.953(10)	5.46	2.80
200	5.1418(1)	10.1952(2)	8.1287(1)	91.831(2)	425.906(10)	5.29	2.78
250	5.1443(1)	10.2028(2)	8.1370(2)	91.682(2)	426.899(10)	5.41	2.74
300	5.1467(1)	10.2103(2)	8.1455(2)	91.510(2)	427.892(10)	5.28	2.73
301	5.1469(1)	10.2118(2)	8.1469(2)	91.491(2)	428.048(10)	4.66	2.77
305	5.1471(1)	10.2117(2)	8.1475(1)	91.485(2)	428.098(9)	4.71	2.60
333	5.1483(1)	10.2167(2)	8.1524(2)	91.361(2)	428.683(9)	4.32	2.26
368	5.1501(1)	10.2222(2)	8.1589(2)	91.186(1)	429.434(9)	5.59	2.82
373	5.1504(1)	10.2231(2)	8.1601(2)	91.148(2)	429.572(11)	4.60	2.74
373	5.1500(1)	10.2231(2)	8.1598(2)	91.147(2)	429.520(11)	4.62	2.60
400	5.1520(1)	10.2274(2)	8.1653(2)	90.967(2)	430.182(10)	4.69	2.43
423	5.1529(1)	10.2312(2)	8.1695(2)	99.781(2)	430.663(12)	4.86	2.42
423	5.1529(1)	10.2312(2)	8.1695(2)	90.783(2)	430.662(13)	4.74	2.49
423	5.1528(1)	10.2311(2)	8.1692(2)	90.766(2)	430.633(13)	4.88	2.76
448	5.1543(1)	10.2352(3)	8.1743(2)	90.463(2)	431.217(15)	4.97	2.25
448	5.1540(2)	10.2347(3)	8.1739(2)	90.439(2)	431.152(14)	4.90	2.38
483	8.1808(3)	5.1555(1)	10.2414(3)		431.945(18)	5.82	2.43
483	8.1810(3)	5.1554(1)	10.2412(3)		431.939(15)	5.31	2.03
500	8.1847(2)	5.1568(1)	10.2443(3)		432.382(15)	5.62	2.20
523	8.1892(2)	5.1580(1)	10.2486(3)		432.905(15)	5.37	2.15
523	8.1893(2)	5.1579(1)	10.2485(3)		432.892(14)	5.17	1.99
573	8.1954(2)	5.1584(1)	10.2524(3)		433.427(14)	5.14	2.08
$CeCu_6$							
10	5.0841(1)	10.1279(2)	8.0731(1)	91.442(1)	415.562(8)	4.71	2.61
50	5.0861(1)	10.1284(2)	8.0740(1)	91.341(1)	415.811(8)	4.83	2.85
100	5.0892(1)	10.1326(2)	8.0789(1)	91.148(1)	416.525(9)	4.83	2.65
150	5.0921(1)	10.1395(2)	8.0860(2)	90.896(2)	417.443(9)	5.08	2.70
175	5.0936(1)	10.1428(2)	8.0893(2)	90.736(2)	417.891(9)	4.89	2.62
200	5.0950(1)	10.1466(2)	8.0931(2)	90.485(2)	418.376(10)	5.03	2.64
250	8.1009(2)	5.0978(1)	10.1548(2)		419.358(11)	5.86	2.60
295	8.1088(2)	5.1004(1)	10.1621(2)		420.286(12)	5.86	2.62
$PrCu_6$							
15	5.0736(1)	10.1157(1)	8.0550(1)	91.487(1)	413.274(7)	4.30	1.95
50	5.0750(1)	10.1142(1)	8.0567(1)	91.340(1)	413.430(8)	4.31	1.94
100	5.0761(1)	10.1174(2)	8.0816(1)	91.140(1)	413.942(8)	4.37	1.97
150	5.0779(1)	10.1237(2)	8.0686(1)	90.858(1)	414.732(9)	4.57	1.95
200	5.0800(1)	10.1309(2)	8.0762(2)	90.320(2)	415.630(11)	4.98	1.93
250	8.0844(2)	5.0823(1)	10.1386(2)		416.570(11)	5.63	1.89
295	8.0921(2)	5.0845(1)	10.1458(2)		417.445(11)	5.52	1.92

TABLE II—*Continued*

T(K)	a(Å)	b(Å)	c(Å)	β(deg.)	V(Å^3)	R_{wp}	R_{exp}
$NdCu_6$							
10	5.0568(1)	10.0933(2)	8.0400(2)	91.163(2)	410.273(11)	4.43	3.42
25	5.0569(1)	10.0935(2)	8.0403(2)	91.130(2)	410.314(11)	4.47	3.40
50	5.0573(1)	10.0937(2)	8.0421(2)	91.019(2)	410.456(12)	4.62	3.52
75	5.0576(1)	10.0954(2)	8.0438(2)	90.898(2)	410.655(12)	4.50	3.41
100	5.0583(1)	10.0983(3)	8.0472(2)	90.699(2)	411.021(13)	4.64	3.49
125	5.0592(1)	10.1004(3)	8.0496(2)	90.536(2)	411.319(13)	4.59	3.43
150	8.0533(3)	5.0596(2)	10.1040(4)		411.700(17)	5.82	3.30
200	8.0609(2)	5.0620(1)	10.1109(3)		412.564(14)	5.22	3.32
250	8.0686(2)	5.0646(1)	10.1180(3)		413.466(13)	5.00	3.28
300	8.0777(2)	5.0672(1)	10.1268(3)		414.503(12)	4.46	2.79

Note. The structure is monoclinic $P2_1/c$ in the low-temperature phase and orthorhombic, *Pnma*, in the high-temperature phase. Both space groups are expressed in the standard settings. R_{wp} is the weighted profile R value; R_{exp} is the expected R value based on counting statistics.

TABLE III

FRACTIONAL ATOMIC POSITIONS AND ISOTROPIC DISPLACEMENT PARAMETERS (Å^2) OF THE $RECu_6$ COMPOUNDS AT THE HIGHEST TEMPERATURE IN THE ORTHORHOMBIC *Pnma* SPACE GROUP AND AT THE LOWEST TEMPERATURE IN THE MONOCLINIC $P2_1/c$ SPACE GROUP

Atom	x	y	z	B	Atom	x	y	z	B
$LaCu_6$			573 K				15 K		
La	0.2600(6)	0.25	0.4365(5)	1.94(12)	La	0.2631(6)	0.4370(3)	0.2619(3)	−0.01(4)
Cu1	0.4344(4)	0.0098(7)	0.1895(4)	1.83(11)	Cu1	0.0092(5)	0.1883(3)	0.4375(3)	−0.07(4)
Cu2	0.1464(6)	0.25	0.1421(5)	2.32(13)	Cu2	0.2390(5)	0.1419(3)	0.1486(3)	0.08(4)
Cu3	−0.1820(6)	0.25	−0.2454(5)	1.95(12)	Cu3	0.2514(5)	−0.2448(3)	−0.1815(4)	0.20(5)
Cu4	−0.4382(8)	0.25	−0.4043(5)	2.77(17)	Cu4	0.2153(5)	−0.4009(2)	−0.4351(3)	0.04(5)
Cu5	−0.1005(6)	0.25	−0.4840(5)	2.23(14)	Cu5	0.2470(5)	−0.4840(2)	−0.1004(4)	0.01(5)
					Cu6	0.5023(6)	−0.1916(3)	−0.4326(4)	0.03(5)
$CeCu_6$			295 K				10 K		
Ce	0.2586(7)	0.25	0.4364(6)	0.79(7)	Ce	0.2550(8)	0.4363(4)	0.2609(4)	0.08(4)
Cu1	0.4350(2)	0.0064(5)	0.1902(1)	0.68(5)	Cu1	0.0070(9)	0.1897(3)	0.4363(3)	0.13(4)
Cu2	0.1476(4)	0.25	0.1432(3)	0.81(6)	Cu2	0.2454(5)	0.1431(2)	0.1462(3)	0.12(3)
Cu3	−0.1813(4)	0.25	−0.2454(3)	0.70(6)	Cu3	0.2520(5)	−0.2445(2)	−0.1813(3)	0.07(3)
Cu4	−0.4397(5)	0.25	−0.4038(3)	1.12(7)	Cu4	0.2278(5)	−0.4021(2)	−0.4382(3)	0.02(4)
Cu5	−0.1000(4)	0.25	−0.4836(3)	0.78(6)	Cu5	0.2495(5)	−0.4849(2)	−0.0998(3)	0.21(4)
					Cu6	0.5024(5)	−0.1917(3)	−0.4321(3)	0.21(4)
$PrCu_6$			295 K				15 K		
Pr	0.2578(8)	0.25	0.4372(7)	1.04(7)	Pr	0.2547(8)	0.4359(4)	0.2612(4)	0.32(4)
Cu1	0.4355(2)	0.0082(5)	0.1902(3)	0.45(4)	Cu1	0.0089(4)	0.1886(2)	0.4374(3)	−0.05(4)
Cu2	0.1470(4)	0.25	0.1431(3)	0.68(6)	Cu2	0.2450(5)	0.1428(2)	0.1473(3)	0.15(3)
Cu3	−0.1807(4)	0.25	−0.2442(3)	0.41(6)	Cu3	0.2500(4)	−0.2442(2)	−0.1815(3)	−0.02(3)
Cu4	−0.4405(5)	0.25	−0.4046(3)	0.97(7)	Cu4	0.2260(4)	−0.4029(2)	−0.4378(3)	0.06(4)
Cu5	−0.0994(4)	0.25	−0.4835(3)	0.61(6)	Cu5	0.2501(4)	−0.4841(2)	−0.1002(3)	−0.02(4)
					Cu6	0.5031(4)	−0.1920(3)	−0.4319(3)	0.22(4)
$NdCu_6$			300 K				10 K		
Nd	0.2610(5)	0.25	0.4365(5)	0.39(6)	Nd	0.2587(8)	0.4370(4)	0.2610(4)	−0.04(5)
Cu1	0.4365(3)	0.0088(6)	0.1908(3)	0.33(5)	Cu1	0.0056(6)	0.1902(4)	0.4361(4)	−0.14(6)
Cu2	0.1459(5)	0.25	0.1415(3)	0.47(6)	Cu2	0.2442(7)	0.1422(3)	0.1466(4)	0.07(6)
Cu3	−0.1824(5)	0.25	−0.2441(4)	0.38(6)	Cu3	0.2497(7)	−0.2443(3)	−0.1819(4)	0.07(6)
Cu4	−0.4391(6)	0.25	−0.4038(4)	0.95(7)	Cu4	0.2329(7)	−0.4034(3)	−0.4387(5)	0.17(6)
Cu5	−0.0986(5)	0.25	−0.4837(4)	0.49(6)	Cu5	0.2510(7)	−0.4836(3)	−0.1003(4)	−0.08(6)
					Cu6	0.5039(7)	−0.1916(4)	−0.4338(4)	0.11(6)

perature according to compound. (Parameters for the other temperatures can be obtained from the authors.) Both the orthorhombic and monoclinic structures are described in their standard settings, which introduces a permutation of axes.

Results and Discussion

Structural Transition

Figures 2a and 2b illustrate a projection of the unit cell of $CeCu_6$ along the orthorhombic **b** (monoclinic **c**) axis. From this figure, and as noted elsewhere (*20*), it can be seen that the atomic displacements associated with the transition consist of a shear along the crystallographic **a** direction in the monoclinic setting with a small amount of atomic displacement perpendicular to the shear direction. This perpendicular displacement is greatest for the Cu4 atom. In $LaCu_6$, where the structural transition occurs at the highest temperature, the perpendicular displacement of the Cu4 atom was 0.1830 Å at 10 K. From Table III, it can also be seen that the Cu4 atom shows the largest decrease in its thermal parameters on going from high to low temperatures. While this suggests that the Cu4 atom could play some role in triggering the transition, a more detailed examination of the anharmonic components of the vibrations of this atom would be needed to confirm this hypothesis.

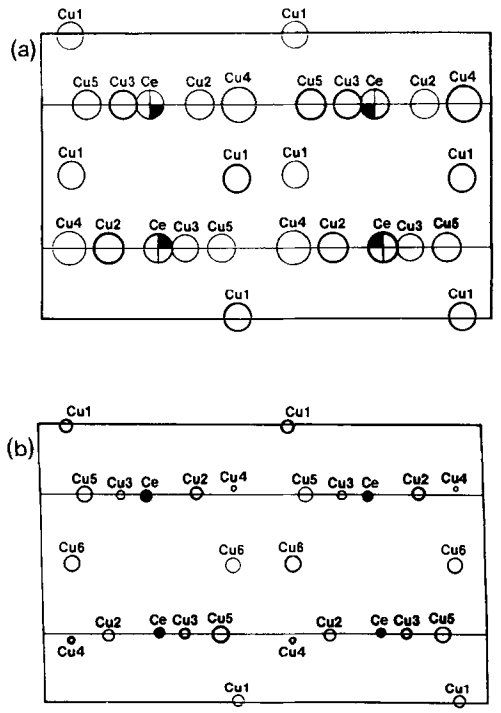

FIG. 2. Projection of the $CeCu_6$ structure along the orthorhombic **c** (monoclinic **b**)-axis. The straight lines at $y = \frac{1}{4}$ and $\frac{3}{4}$ mark the planes in which all atoms except Cu1 are located in the high-temperature orthorhombic structure. (a) Above the transition $T = 295$ K; (b) below the transition $T = 10$ K.

Within the precision of this measurement, the lattice parameters and the unit cell volume of all of the $RECu_6$ compounds studied show smooth changes versus temperature, supporting the hypothesis (*15*, *18–20*) of a continuous transition. Landau theory allows the transition from *Pnma* to $P2_1/c$ to be second order with a proper order parameter being the monoclinic strain $ac\cdot\cos\beta$. With the values of a, c, and β obtained from the Rietveld structural refinements (Table II), a plot of the order parameter as a function of reduced temperature T/T_0 can be drawn. To determine the transition temperature for each compound, the data were least-squares fit to a three-parameter equation of the form

$$ac\cdot\cos\beta = A(1 - T/T_0)^{\eta},$$

where A is the constant for the transition, T_0 is the transition temperature, and η is the exponent for the transition. Mean field theory would require the values for η to be exactly $\frac{1}{2}$, but a more sensible estimate of the transition temperature is obtained if the exponent is allowed to vary. The deviation from $\frac{1}{2}$ is possibly due to the large temperature range, extending far outside the critical region of the transition, over which the data

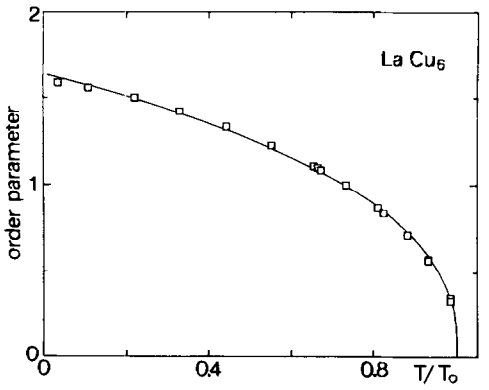

FIG. 3. The monoclinic strain (ac·cos β) vs reduced temperature for $LaCu_6$. The solid line is a least-squares fit to the data according to the three-parameter equation provided in the text.

were collected. Thus the precision of these data do not warrant an interpretation of their exponent in terms of a critical exponent. Figure 3 displays the results of fitting this equation to the temperature dependence of the order parameter obtained from the $LaCu_6$ data. Table IV lists the calculated transition temperatures and the values for η obtained for each compound. These results are comparable to those reported by Yamada *et al.* (*15*) who took twice the monoclinic deviation angle, $\delta(T)$, as the order parameter for the transition. They found $\eta = 0.44$ for $CeCu_6$ and $\eta = 0.43$ for $LaCu_6$.

Comparison of the Rare Earth Compounds

The structural refinements of the lattice parameters allow a direct comparison of lattice constants with the ionic size of the rare earth element in each compound. In Fig. 4, we plot rare earth number versus the room temperature value of $|\mathbf{b}|$ (which is expected to be most affected by the rare earth ionic radius). A systematic decrease in size of the rare earth ion as one progresses across the La–Ce–Pr–Nd series is a manifestation of the lanthanide contraction. The observed axis lengths, $|\mathbf{b}|$, show a deviation from an expected linear decrease based on the assumption of a constant oxidation number. Similar observations have been made in other studies of the rare earth series (e.g., *26*) and this deviation is generally attributed to the cerium ion (and to a lesser extent the praseodymium ion) having nontrivalent formal oxidation number. Unfortunately, without comparable data from other $RECu_6$ compounds, it is impossible to conclude unambiguously which points in Fig. 4 are anomalous.

It is also interesting to compare the structural transition temperatures of the $RECu_6$ compounds. The curve corresponding to the righthand scale of Fig. 4 shows a plot of the transition temperature for each compound as a function of its corresponding room temperature lattice constant $|\mathbf{b}|$. If we

TABLE IV

THE STRUCTURAL PHASE TRANSITION TEMPERATURES AND EXPONENTS FROM THE FIT OF THE POWDER NEUTRON DIFFRACTION DATA TAKEN ON THE $RECu_6$ COMPOUNDS

Sample	$\eta = \frac{1}{2}$	η varied	
	T_0	T_0	η
$LaCu_6$	491 ± 19 K	454.7 ± 1.0 K	0.387 ± 0.007
$CeCu_6$	230 ± 9 K	213.8 ± 1.8 K	0.407 ± 0.015
$PrCu_6$	212 ± 6 K	206.0 ± 0.9 K	0.443 ± 0.014
$NdCu_6$	155 ± 7 K	150.6 ± 11.0 K	0.471 ± 0.087

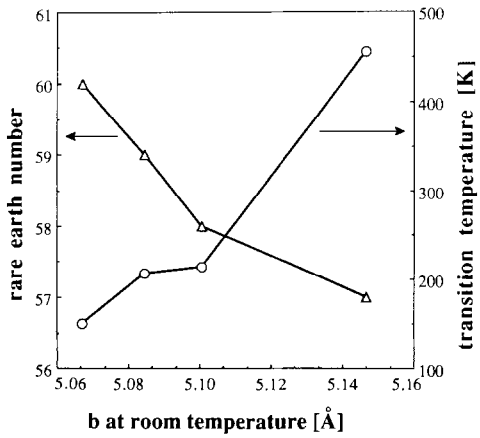

FIG. 4. The rare earth number vs room temperature lattice constant |**b**| for the $RECu_6$ compounds on the lefthand side and the structural transition temperature vs room temperature lattice constant |**b**| on the right-hand side.

assume that the interatomic forces are the same in each of these systems, the transition temperature should roughly scale with the rare earth ionic radius. $CeCu_6$ again deviates significantly from this behavior, suggesting that the coulomb forces acting on the cerium ion are somewhat different than those acting on the rare earth ions in the other systems. The simplest explanation for this would be that the cerium is in a different formal oxidation state, causing the force constants to be slightly modified in this material.

Conclusion

Analysis of the powder neutron diffraction data has provided details of the structural phase transition found in $RECu_6$ compounds, where RE = La, Ce, Pr, and Nd. In all four compounds, our observations are consistent with a second-order phase transition with the proper order parameter being the monoclinic strain $ac\cdot\cos\beta$. Using data collected over a wide range of temperatures in the monoclinic phase, the transition temperature for each compound was most accurately determined by performing a least-squares fit allowing both the transition temperature and the exponent for the transition to vary. Since in all cases, the temperature range of the data collection extended considerably beyond the critical region of the transition, we do not expect this exponent to be a true critical exponent for the transition. Comparison of the values of |**b**| for the unit cell of the different $RECu_6$ compounds to the corresponding rare earth number gave evidence that the formal oxidation state of the cerium ion is greater than three. When the values of |**b**| are then compared as a function of their transition temperature, we are able to speculate that the driving mechanism for the phase transition is the same in all the $RECu_6$ compounds studied.

References

1. Y. ONUKI, M. NISHIHARA, Y. FUJIMURA, T. YAMAZAKI, AND T. KOMATSUBARA, *J. Magn. Magn. Mater.* **63/64,** 317 (1987).
2. T. FUJITA, K. SATOH, Y. ONUKI, AND T. KOMATSUBARA, *J. Magn. Magn. Mater,* **47/48,** 66 (1985).
3. H. R. OTT, H. RUDIGIER, Z. FISK, J. O. WILLIS, AND G. R. STEWART, *Solid State Commun.* **53,** 235 (1985).
4. G. R. STEWART, Z. FISK, AND M. S. WIRE, *Phys. Rev. B* **30,** 482 (1984).
5. Y. ONUKI, Y. SHIMIZU, AND T. KOMATSUBARA, *J. Phys. Soc. Japan* **54,** 304 (1985).
6. S. ZEMIRLI AND B. BARBARA, *Solid State Commun.* **56,** 385 (1985).
7. A. SUMIYAMA, Y. ODA, H. NAGANO, Y. ONUKI, AND T. KOMATSUBARA, *J. Phys. Soc. Japan* **54,** 877 (1985).
8. Y. ONUKI, Y. SHIMIZU, T. KOMATSUBARA, A. SUMIYAMA, Y. ODA, H. NAGANO, T. FUJITA, Y. MAENO, K. SATOH, AND T. OHTSUKA, *J. Magn. Magn. Mater.* **52,** 344 (1985).
9. A. AMATO, D. JACCARD, E. WALKER, AND J. FLOUQUET, *Solid State Commun.* **55,** 1131 (1985).
10. A. SUMIYAMA, Y. ODA, H. NAGANO, Y. ONUKI, K. SHIBUTANI, AND T. KOMATSUBARA, *J. Phys. Soc. Japan* **55,** 3155 (1985).
11. J. KIELY, T. MANLEY, R. PONTINEN, AND W. WEYHMAN, *J. Appl. Phys.* **52,** 2104 (1981).
12. J. BABCOCK, J. KIELY, T. MANLEY, AND W. WEYHMAN, *Phys. Rev. Lett.* **43,** 380 (1979).

13. Y. ONUKI, K. IRA, M. NISHIHARA, T. KOMATSUBARA, S. TAKAYANAGI, K. KAMEDA, AND N. NADA, *J. Phys. Soc. Japan* **55,** 1818 (1986).
14. H. ASANO, M. UMINO, Y. HATAOKA, Y. SHIMIZU, Y. ONUKI, T. KOMATSUBARA, AND F. IZUMI, *J. Phys. Soc. Japan* **54,** 3358 (1985).
15. K. YAMADA, I. HIROSAWA, Y. NODA, Y. ENDOH, Y. ONUKI, AND T. KOMATSUBARA, *J. Phys. Soc. Japan* **56,** 3553 (1987).
16. T. SUZUKI, T. GOTO, A. TAMAKI, T. FUJIMURA, Y. ONUKI, AND T. KOMATSUBARA, *J. Phys. Soc. Japan* **54,** 2367 (1985).
17. T. GOTO, T. SUZUKI, A. TAMAKI, T. FUJIMURA, Y. ONUKI, AND T. KOMATSUBARA, *J. Magn. Magn. Mater.* **63/64,** 3098 (1987).
18. Y. NODA, K. YAMADA, I. HIROSAWA, Y. ENDOH, Y. ONUKI, AND T. KOMATSUBARA, *J. Phys. Soc. Japan* **54,** 448 (1985).
19. E. GRATZ, E. BAUER, H. NOWOTNY, H. MUELLER, S. ZEMIRLI, AND B. BARBARA, *J. Magn. Magn. Mater.* **63/64,** 79 (1987).
20. M. L. VRTIS, J. D. JORGENSEN, AND D. G. HINKS, *Physica* **136B,** 489 (1986).
21. H. ASANO, M. UMINO, Y. ONUKI, T. KOMATSUBARA, F. IZUMI, AND N. WATANABE, *J. Phys. Soc. Japan* **56,** 2245 (1987).
22. J. D. JORGENSEN AND J. FABER JR., *in* "Sixth Meeting of the International Collaboration on Advanced Neutron Sources," 105 Argonne National Laboratory, Report No. ANL-82-80 (1983).
23. R. B. VON DREELE, J. D. JORGENSEN, AND C. G. WINDSOR, *J. Appl. Crystallogr.* **15,** 581 (1982).
24. D. T. CROMER, A. C. LARSON, AND R. B. ROOF JR., *Acta Crystallogr.* **13,** 913 (1960).
25. K. H. J. BUSCHOW AND A. S. VAN DER GOOT, *J. Less-Common Met.* **20,** 309 (1970).
26. B. JOHANSSON AND A. ROSENGREN, *Phys. Rev. B* **11,** 2836 (1975).